NASA TECHNICAL MEMORANDUM

NASA TM X-64923

(NASA-TM-X-64923) KINETIC STUDIES OF THE STRESS CORROSION CRACKING OF D6AC STEEL (NASA) 27 p HC $3.75 CSCL 11F

N75-21434

Unclas

G3/26 19391

KINETIC STUDIES OF THE STRESS CORROSION CRACKING OF D6AC STEEL

By Pascal J. Noronha
Materials and Processes Laboratory

March 25, 1975

NASA

George C. Marshall Space Flight Center
Marshall Space Flight Center, Alabama

MSFC - Form 3190 (Rev June 1971)

TECHNICAL REPORT STANDARD TITLE PAGE

1. REPORT NO.	2. GOVERNMENT ACCESSION NO.	3. RECIPIENT'S CATALOG NO.
NASA TM X-64923		

4. TITLE AND SUBTITLE	5. REPORT DATE
Kinetic Studies of the Stress Corrosion Cracking of D6AC Steel	March 25, 1975
	6. PERFORMING ORGANIZATION CODE
7. AUTHOR(S)	8. PERFORMING ORGANIZATION REPORT #
Pascal J. Noronha	
9. PERFORMING ORGANIZATION NAME AND ADDRESS	10. WORK UNIT NO.
George C. Marshall Space Flight Center Marshall Space Flight Center, Alabama 35812	11. CONTRACT OR GRANT NO.
	13. TYPE OF REPORT & PERIOD COVERED
12. SPONSORING AGENCY NAME AND ADDRESS	
National Aeronautics and Space Administration Washington, D.C. 20546	Technical Memorandum
	14. SPONSORING AGENCY CODE

15. SUPPLEMENTARY NOTES

Prepared by Materials and Processes Laboratory, Science and Engineering

16. ABSTRACT

A study was conducted to determine the effect of load interactions on the crack growth velocity of D6AC steel under stress corrosion cracking conditions, from which the results will be used to obtain realistic lifetimes of D6AC structures. The environment was a 3.5 percent salt solution. The modified wedge opening load specimens were fatigue precracked and subjected to a deadweight loading in creep machines. The effects of load shedding on incubation times and crack growth rates were measured using high-sensitivity compliance measurement techniques. Load shedding results in an incubation time, the length of which depends on the amount of load shed and the baseline stress intensity. The sequence of unloading the specimen also controls the subsequent incubation period. The incubation period is shorter when load shedding passes through zero load than when it does not if the specimen initially had the same baseline stress intensity. The crack growth rates following the incubation period are also different from the steady-state crack growth rate at the operating stress intensity. Based on these data, it appears that the susceptibility of this alloy system to stress corrosion cracking depends on the plane-strain fracture toughness and on the yield strength of the material.

17. KEY WORDS	18. DISTRIBUTION STATEMENT
	Unclassified-unlimited E. C. McKannan E. C. McKANNAN

19. SECURITY CLASSIF. (of this report)	20. SECURITY CLASSIF. (of this page)	21. NO. OF PAGES	22. PRICE
Unclassified	Unclassified	28	NTIS

TABLE OF CONTENTS

	Page
INTRODUCTION	1
EXPERIMENTAL PROCEDURES	2
RESULTS AND DISCUSSION	5
CONCLUSIONS	9
REFERENCES	10

LIST OF ILLUSTRATIONS

Figure	Title	Page
1.	Detailed machine drawing for modified wedge-open-loaded specimen	12
2.	Flow diagram for stress intensities applied to specimen	13
3.	Block diagram of experimental technique	14
4.	Tracing of recorder plot showing steady-state growth and crack arrest	15
5.	Initial incubation times as a function of initial stress intensity	17
6.	Crack growth rate versus stress intensity in 3.5 percent salt solution	18
7.	Incubation times for load shed not passing through zero load from a steady-state condition of crack growth	19
8.	Incubation times for load shed passing through zero load from a steady-state condition of crack growth	20
9.	Ratio of stress intensities vs square root of time for incubation after load shedding not passing through zero load	21
10.	Crack growth rates following incubation vs load shed not passing through zero load	22

LIST OF TABLES

Table	Title	Page
1.	Composition of D6AC Steel	2
2.	Mechanical Properties of D6AC Steel	3
3.	Comparison of Crack Growth Rates for Different Yield Strengths in 4340 Steel in 3.5 Percent Salt Solution	6

TECHNICAL MEMORANDUM X-64923

KINETIC STUDIES OF THE STRESS CORROSION CRACKING OF D6AC STEEL

INTRODUCTION

Environmentally enhanced crack growth in high-strength steels has been observed by many investigators. To prevent the premature failure of structures, particularly those that may undergo combinations of varying load levels and stress corrosion cracking environments, the phenomena of subcritical crack growth in the presence of the corrosive environment must be characterized.

With the advent of fracture mechanics concepts, the crack tip stress intensity factor, K_I, has been shown to be an appropriate parameter to characterize the mechanical driving forces for environmentally enhanced crack growth. In the development of techniques and understanding about the roll of the stress intensity factor in stress corrosion cracking, the initial investigations were concerned with the measurement of the onset of growth [1,2]. Later investigations dealt with the development of the threshold stress intensity factors associated with the stress corrosion cracking process, K_{ISCC} [3-5]. The most recent phase of stress corrosion studies is concerned with the kinetics of the crack growth rates (da/dt) as a function of the applied stress intensity factor, K_I. This has been investigated in steels for a variety of environments and loading conditions [6-8].

Although crack initiation times and crack growth rates are the two important factors in determining the life of an engineering structure, recent work indicates that there are others. Harrigan, Dull, and Raymond [9] show that steady-state crack growth under deadweight loading may be arrested by load level changes, thus enhancing useful life. For critical engineering structures, fracture mechanics design concepts must assume the presence of a defect in the structure. Thus, for a conservative estimate of the useful life of a structure under stress corrosion conditions, one cannot include the crack initiation period of the stress corrosion cracking process. The safe life of a

structure may be decreased in proportion to the number and types of defects present. For a critical structure, this results in the use of a high factor of safety based on yield strength. To make a realistic estimate of the safe life of such a structure, it becomes necessary to determine crack growth rates and intermediate arrest times caused by load level changes. If, for example, reduction of the load level causes crack arrest due to a decrease in the stress intensity K_{I_i} at the crack tip, the safe life of the structure is enhanced by the duration of the incubation time before resumption of crack growth. Conversely, an increase in the load level may result in a crack growth rate higher than the steady-state growth rate at the operating stress intensity. This study was conducted on D6AC steel to determine the effect of changes in load levels on the incubation times and subsequent crack growth rates.

EXPERIMENTAL PROCEDURES

This study used D6AC steel specimens machined from the plate form such that the crack plane was parallel to the short transverse direction, with crack propagation occurring in the longitudinal direction. The composition of the specimens is shown in Table 1, and a detailed description of the specimens is shown in Figure 1. The specimens had the modified wedge-open-loaded configuration suggested by Novak and Rolfe [10] and a nominal thickness of 12.7 mm (0.5 in.). This thickness was less than that specified by Brown and and Srawley [11],

$$B/(K_{IC}/\sigma_{YS})^2 \geq 2.5 \quad , \tag{1}$$

for obtaining plane strain conditions at the crack tip.

TABLE 1. COMPOSITION OF D6AC STEEL

Element	C	Mn	P	S	Si	Ni	Cr	Mo	Va
Percentage	0.48	0.75	0.006	0.006	0.26	0.56	1.09	1.00	0.08

The D6AC specimens were treated to a hardness of Rc44. This was accomplished by an initial normalization at 940°C (1725°F) for 30 minutes followed by cooling to room temperature, tempering at 677°C (1250°F) for

1.5 hours, then cooling to room temperature. This was followed by austenizing at 885°C (1625°F), quenching into 204°C (400°F) salt with agitation, stress relieving at 204°C for 1 hour in a salt bath, and double tempering at 621°C (1150°F) for 2 hours to obtain the required mechanical properties. The resulting mechanical properties are shown in Table 2.

TABLE 2. MECHANICAL PROPERTIES OF D6AC STEEL

Property	Transverse	Longitudinal
Tensile Strength [kg/cm^2 (ksi)]	13 175 (187)	13 034 (185)
Yield Strength [kg/cm^2 (ksi)]	12 365 (175.5)	12 294 (174.5)
Percent Elongation in 5.08 cm (2 in.)	12.3	12.3
Modulus $\times 10^{-6}$ kg/cm^2 (10^{-6} psi)	2.128 (30.2)	2.226 (31.6)
Hardness Rc	44	44
K_Q [$MN/m^{3/2}$ (ksi $\sqrt{in.}$)]	93.5 (85)	
K_{ISCC} [$MN/m^{3/2}$ (ksi $\sqrt{in.}$)]	21.45 (19.5)	

The specimens were fatigue precracked 2.54 mm (0.10 in.) past the machined starter notch, and the stress intensity for precracking was always below 20.9 $MN/m^{3/2}$ (19 ksi $\sqrt{in.}$) or below K_{ISCC}. This ensured that the fatigue loads that were applied in no way affected the kinetics of stress corrosion of the specimen. Figure 2 shows the flow diagrams of the stress intensity loading sequence of the specimens. The fatigue precracking in air was followed by loading of the specimen in a creep machine with environment present at the tip of the crack. The specimens were loaded to an initial stress intensity and the initial incubation time prior to stress corrosion cracking was determined. As cracking occurred, the stress intensity increased under constant load. After a steady-state crack growth condition was achieved, load shedding was done in either of two ways. In the first method (Fig. 2a), load shedding was achieved by removal of the required load to give a reduction of the stress intensity of ΔK. The final stress intensity on removal of the load was K_F, which resulted in the presence of an incubation period followed by crack

extension. In the second sequence (Fig. 2b), a steady-state crack growth rate was achieved as in the first case, followed by load shedding. In this case, however, the load was reduced to zero from its original value of stress intensity at which steady-state crack growth occurred, and then was increased to the value K_F, which was below the original value by an amount of ΔK. On the application of the load required for K_F, this sequence also resulted in an incubation time followed by crack extension. In both cases, the steady-state growth condition was achieved after a crack arrest period.

Incubation times and crack growth rates were obtained by the use of compliance techniques. The system used for measuring crack opening displacement is shown in Figure 3. It consists of a NASA-type clip gage, excited at 10 Vdc. The output from the clip gage is fed into a Dana high-gain amplifier. After amplification, the signal is coupled to the y-axis of a Hewlett-Packard x-y recorder. The sensitivity of the components in the system was adjusted to allow a 0.0254 mm (0.001 in.) increase in crack opening displacement to be magnified to 5.24 cm (6 in.) of displacement, or greater, of the recorder pen on the y-axis. The x-axis was coupled to a ramp generator to allow 8.1 cm (15 in.) displacement of the pen to correspond to 24 hours. This arrangement allowed crack opening displacement to be monitored versus time.

An accurate tracing of one of the results obtained is shown in Figure 4. Steady-state crack extension is seen on the left, followed by load shedding resulting in a decrease in the crack opening displacement. The flat portion corresponds to the incubation time, with the start of crack extension corresponding to the discontinuous portion of the curve. In nearly all cases, the start of crack extension was discontinuous, and the incubation time was measured to within 1 percent. All drift over a 24 hour period and greater was eliminated so that no extrapolation techniques were required for analysis.

Crack growth rates were obtained from crack opening displacement measurements, using compliance techniques as described by Novak and Rolfe [10]. The compliance values of $C_3(a/w)$ and $C_6(a/w)$ developed for the D6AC steel modified wedge-open-loaded specimens are:

$$C_3(a/w) = 30.96(a/w) - 195.8(a/w)^2 + 730.6(a/w)^3 - 1186(a/w)^4 + 754.6(a/w)^5 \quad \text{--- (i)}$$

$$C_6(a/w) = e^{2.255964 + 1.65021(a/w) + 12.974822(a/w)^2 - 26.02392(a/w)^3 + 18.36501(a/w)^4}$$

RESULTS AND DISCUSSION

In most studies of stress corrosion crack growth rates, it is generally assumed that the driving force in terms of the instantaneous stress intensity, K_I, is invariant with respect to time for constant values of K. This is certainly true for crack growth rates (da/dt) obtained from steady-state studies. It is not as straightforward for stress corrosion conditions where there have been load level changes.

Even under the constant loading conditions, subcritical crack growth has several stages: incubation period, crack acceleration, steady-state crack growth, and catastrophic propagation to failure. With the presence of load interactions, each of these stages undergoes a change. Therefore, the use of time-to-failure curves for stress corrosion cracking processes may lead to incorrect estimates of the structural life if the material is strongly dependent upon the prestress levels.

Figure 5 shows the incubation times associated with rising stress intensity factors. In each case the specimen was precracked with a maximum stress intensity factor of 20.9 $MN/m^{3/2}$ (19 $ksi\sqrt{in.}$) in dry air, the environment was then added, and the specimen was loaded to the final experimental stress intensity factor. Figure 5 shows that the incubation times decreased from a value of 18 hours for an applied stress intensity of 38.5 $MN/m^{3/2}$ (35 $ksi\sqrt{in.}$) to less than 15 minutes for an applied stress intensity factor of 82.5 $MN/m^{3/2}$ (75 $ksi\sqrt{in.}$). This is in contrast to the results of Williams [12] who reports an incubation period for subcritical crack growth in TI-4Al-3Mo-1V to be independent of initial stress intensity. In this work it should be noted that the incubation time is given as the time to the first measurable change in the compliance-versus-time curve. Since the system is extremely sensitive and capable of detecting almost infinitesimal crack growth over short periods, the incubation times are not equatable to the normal definition of less than 2.54×10^{-6} cm (10^{-6} in.) per hour. For the condition of the presence of a defect (a crack) in the material, under stress corrosion conditions, it is apparent that initiation of crack growth occurs in relatively short periods. This is different from the situation of no defect present initially, where stress corrosion crack growth can occur only after a defect has been introduced — generally by pitting or crevice corrosion. The times required for the defect to be introduced and for cracking to be initiated by these processes are much greater in comparison with the incubation times in Figure 5. This serves to

illustrate that by using conservative design criteria by assuming the presence of a defect in the material, the useful life of a structure is considerably reduced under stress corrosion cracking conditions.

The rate of steady-state crack growth in D6AC steel is shown in Figure 6. The deadweight-loaded specimens of this study had a crack growth rate at different stress intensities that were slightly above the rates for identical specimens under wedge-open-loaded conditions. A comparison with the rates of crack growth of D6AC from the study by Harrigan, Dull, and Raymond [9] has also been made. Their rates were for the initial growth rates, before the application of any load interactions, and are higher than those obtained in this study. Even with these differences the changes in crack growth rates under steady-state conditions are not too different. The difference may be attributed in part to the difference in tensile strength and fracture toughness of the parent materials: 15 852 kg/cm^2 (225 ksi) yield and 64.89 ± 6.6 MN/m$^{3/2}$ (59 ± 6 ksi$\sqrt{\text{in.}}$) K_Q for Reference 9 versus 12 330 kg/cm^2 (175 ksi) yield and 93.5 ± 4.4 MN/m$^{3/2}$ (85 ± 4 ksi$\sqrt{\text{in.}}$) K_Q for this study.

A similar conclusion about crack growth rates may be obtained from a comparison of rates for 4340 steels. Based on an analysis of three separate studies [6, 9, 13], it is seen that to a first approximation, the steels with the higher yield strength show higher growth rates at the same stress intensity. All three studies were conducted at room temperature in 3.5 percent salt solution, and the results are shown in Table 3.

TABLE 3. COMPARISON OF CRACK GROWTH RATES FOR DIFFERENT YIELD STRENGTHS IN 4340 STEEL IN 3.5 PERCENT SALT SOLUTION

Reference No.	Yield Strength [kg/cm^2 (ksi)]	Range of Stress Intensities [MN/m$^{3/2}$ (ksi$\sqrt{\text{in.}}$)]	Crack Growth Rates [cm/hr (in./hr)]
10	16 909 (240)	22.0 to 71.5 (20 to 65)	1.27 to 3.2 (0.5 to 1.26)
12	15 218 (216)	22.0 to 55.0 (20 to 50)	0.76 to 2.29 (0.3 to 0.9)
6	14 515 (206)	22.0 to 55.0 (20 to 50)	0.30 to 0.64 (0.12 to 0.25)

Figure 7 shows a plot of the incubation times required for measurable crack growth after shedding load. The curves are plotted as a function of the drop in stress intensity factor. Thus it can be seen that if the drop in stress intensity factor increases (increasing load shedding), the time to propagate the existing crack increases. The two curves are plotted as a function of the baseline stress intensity factor. For the baseline of 93.5 $MN/m^{3/2}$ (85 $ksi\sqrt{in.}$), the loading sequence was as follows:

98.7 to 93.5 $MN/m^{3/2}$ (89.7 to 85 $ksi\sqrt{in.}$)

95.5 to 93.5 $MN/m^{3/2}$ (86.8 to 85 $ksi\sqrt{in.}$)

94.6 to 93.5 $MN/m^{3/2}$ (86 to 85 $ksi\sqrt{in.}$)

94.0 to 93.5 $MN/m^{3/2}$ (85.5 to 85 $ksi\sqrt{in.}$)

The incubation times varied from about 17 minutes to over 50 hours. As would be expected, the incubation times for the base of 95.7 $MN/m^{3/2}$ (87 $ksi\sqrt{in.}$) were shorter than those obtained for the base of 77 $MN/m^{3/2}$ (70 $ksi\sqrt{in.}$), but both curves follow the same trend.

The incubation periods following the load-shedding sequence passing through zero load are shown in Figure 8. It is plotted as the incubation time in hours versus the amount of load shed for a baseline load level of 82.5 $MN/m^{3/2}$ (75 $ksi\sqrt{in.}$). The resulting plot is seen to be a straight line similar to that obtained in Figure 7. One difference, however, is the slope of the line, which is seen to be considerably less than for the case of load shedding not passing through a zero load. Incubation times obtained following this unloading sequence are much lower than for the first sequence, even though the baseline load level of 82.5 $MN/m^{3/2}$ is much lower than for the case of 95.7 $MN/m^{3/2}$ (87 $ksi\sqrt{in.}$). Passing through zero load level reduces the periods of crack arrest, but it is not yet certain why this is so. It is known that the sequence results in a change in the size of the zone of plastic deformation at the tip of the crack and also generates new surfaces at the tip of the crack, since it can be considered as one fatigue cycle. The fracture mechanics approach, however, is a continuous one and does not give information regarding the detailed structural features at the crack tip. However, efforts are now under way to study the phenomenon of stress corrosion cracking by conducting an in-depth study of the kinetics of the process.

A comparison of the load-shedding behavior of the specimens in this study was made with the specimens of the Harrigan et al. study [9]. By plotting the results of the square root of the incubation times versus the value of $\Delta K/K_F$ in Figure 9, an empirical relationship was obtained. Here ΔK is the amount of load shed and K_F, the baseline stress intensity. The empirical relationship of incubation time to the load-shedding ratio for D6AC has the form of

$$\sqrt{t} = 370 \frac{\Delta K}{K_F} - 2.9$$

in hours.

The incubation times for the specimens in this study are longer than for the sames values of $\Delta K/K_F$ in the study of Reference 9. If, for the same alloy system, similar equations can be obtained for incubation periods caused by load shedding, then the constants in the equation are a measure of the retardation to crack growth caused by the load shedding. The specimens in this study show greater resistance to stress corrosion cracking than Harrigan's specimens, which may be attributed to the higher value of the fracture toughness of the specimens in this study. In general, if the value of the critical stress intensity in plane strain is increased and the yield strength correspondingly decreased, the resistance to stress corrosion cracking is increased. The increase in resistance is manifested by longer incubation times both before initial crack growth and after load shedding and by slower rates of steady-state crack growth.

Stress corrosion crack velocity following the end of incubation is plotted in Figure 10 as a function of the amount of load shed for a given baseline load level. The crack growth rates are higher for lower values of load shedding and differ from the results of Marcus and Sih [14]. The slower rates of crack growth obtained with a larger amount of load shed are a trend that is also observed in retardation due to peak overloads in cyclic flaw growth. It is believed that the causes are similar in nature, namely, retardation due to the increased plastic deformation caused by the overload. Their measurements of stress corrosion crack velocity in titanium at differing stress levels show no changes in crack velocity due to load interactions. While going from 250 to 227 kg (550 to 500 lb) and from 273 to 227 kg (600 to 500 lb) for TI-75A in a methanol 0.01N NaCl-0.3 wt. percent aqueous solution, there was no change in

crack propagation rates at the lowered load level. However, it should be recognized that the rates of crack growth discussed by Marcus and Sih are several orders of magnitude faster than those exhibited by the high-strength steels, e.g., 0.003 cm/sec (4.251 in./hour) for Ti-75A versus 0.00508 millicentimeters/hour (2 milliinches/hour) for D6AC steels. Thus the influences of load shedding may not be observable at the faster crack propagation rates, or in proportion may be much smaller than the difference in the rates observed in the D6AC steel.

CONCLUSIONS

The results of this investigation into the behavior of D6AC steel under deadweight-loaded conditions are

1. Load shedding under stress corrosion cracking conditions causes a temporary arrest of growth of the crack.

2. The period of crack arrest depends on the amount of load shed and the baseline stress intensity of the specimen. The greater the amount of load shed, the longer the incubation period, and the higher the baseline stress intensity, the shorter the incubation period for the same level of load shedding.

3. Load shedding, done by passing the specimen through a zero-load condition, namely, the sequence shown in Figure 2b, results in a shorter incubation period than for the same amount of load shedding, using the sequence shown in Figure 2a, which does not pass through zero load.

4. The crack growth rates following incubation caused by load shedding depend on the amount of load shed and the baseline load level. Crack growth rates are lower following greater values of load shedding.

5. The "resistance" to stress corrosion cracking depends on the fracture toughness and yield strength of the specimens of a particular alloy system.

REFERENCES

1. Leiche, H. P.; and Loginow, A. W.: Stress Corrosion Behavior of High Strength Steels. Corrosion, Vol. 24, No. 9, 1968, pp. 291-297.

2. Echel, J. F.: Stress Corrosion Crack Nucleation and Growth in Austenitic Stainless Steels. Corrosion, Vol. 18, 1962, p. 270.

3. Novak, S. R.: Effect of Prior Uniform Plastic Strain on the K_{ISCC} of High-Strength Steels in Sea-Water. Engineering Fracture Mechanics, Vol. 5, 1973, pp. 727-763.

4. Wei, R. P.; Novak, S. R.; and Williams, D. P.: Some Important Considerations in the Development of Stress Corrosion Cracking Test Methods. Materials Research and Standards, Vol. 12, No. 9, 1972, p. 25.

5. Smith, H. R.; Piper, D. E.; and Downey, F. K.: A Study of Stress-Corrosion Cracking by Wedge-Force Loading. Engineering Fracture Mechanics, Vol. 1, 1968, pp. 123-128.

6. Sullivan, A. M.: Stress Corrosion Crack Velocity in 4340 Steel, Engineering Fracture Mechanics, Vol. 4, 1972, pp. 65-76.

7. Carter, C. S.: Stress Corrosion Crack Branching in High-Strength Steels. Engineering Fracture Mechnics, Vol. 3, 1971, pp. 1-13.

8. Williams, D. P.: A New Criterion for Failure of Materials by Environment-Induced Cracking. International Journal of Fracture, Vol. 9, No. 1, Mar. 1973.

9. Harrigan, W. C.; Dull, D. L.; and Raymond, L.: Effect of Loading Sequence on Threshold Stress Intensity Determination. Progress in Flaw Growth and Fracture Toughness Testing, ASTM STP 536, 1973, pp. 171-181.

10. Novak, S. R.; and Rolfe, S. T.: Modified WOL Specimen for K_{ISCC} Environmental Testing. Journal of Materials, Vol. 4, No. 3, Sept. 1969.

REFERENCES (Concluded)

11. Brown, W. F.; and Srawley, J. E.: Plane Strain Crack Toughness Testing of High Strength Metallic Materials. ASTM-STP 410, 1966.

12. Williams, D. N.: Subcritical Crack Growth Under Sustained Load. Metallurgical Transactions, Vol. 5, Nov. 1974, pp. 2351-2358.

13. Van der Sluys, W. A.: Mechanism of Environment Induced Subcritical Flaw Growth in AISI 4340 Steel. Engineering Fracture Mechanics, Vol. 1, 1969, pp. 447-462.

14. Marcus, H. L.; and Sih, G. C.: A Crack Line Loaded Edge Crack Stress Corrosion Specimen. Engineering Fracture Mechanics, Vol. 3, 1971, pp. 453-461.

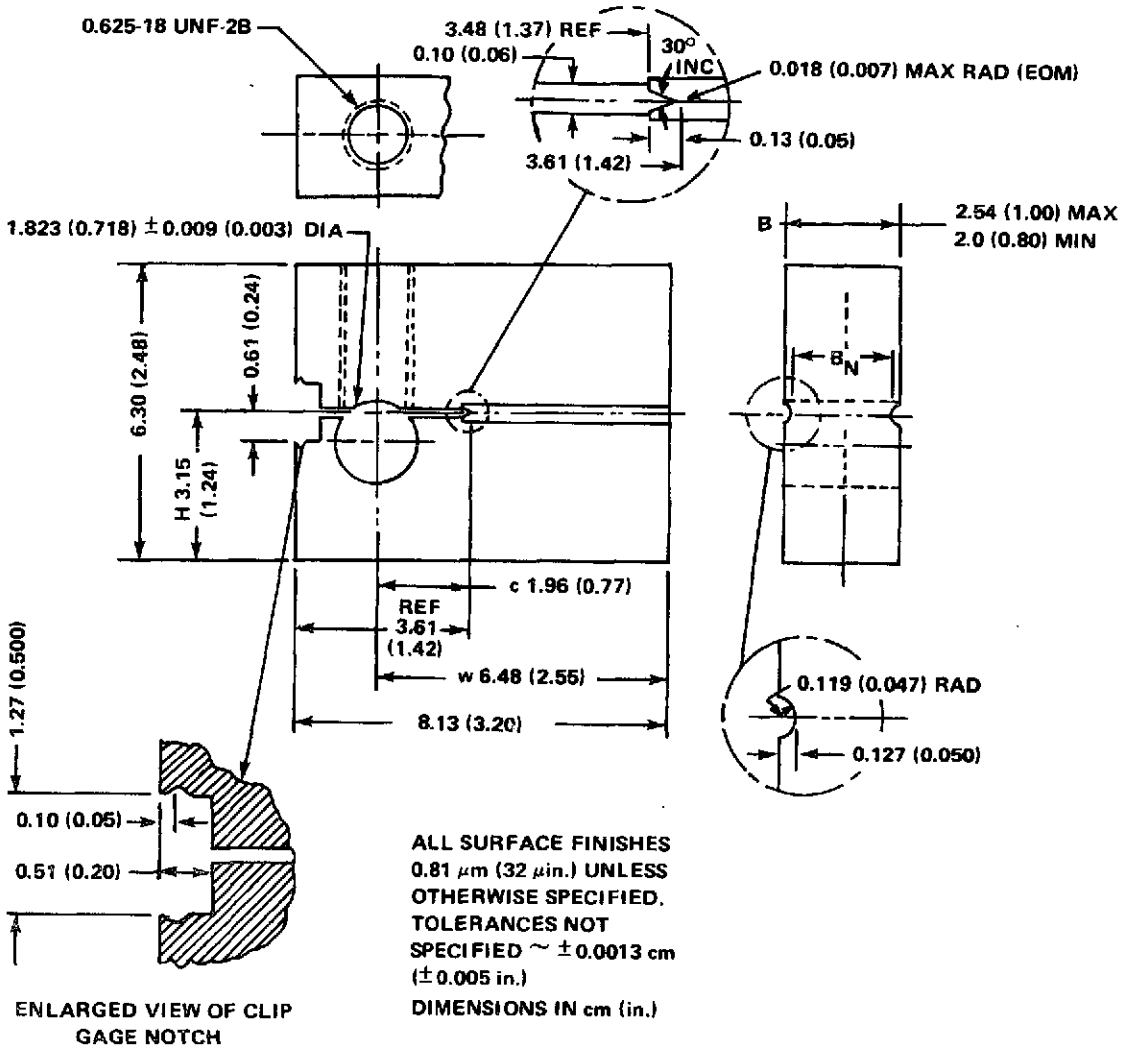

Figure 1. Detailed machine drawing for modified wedge-open-loaded specimen.

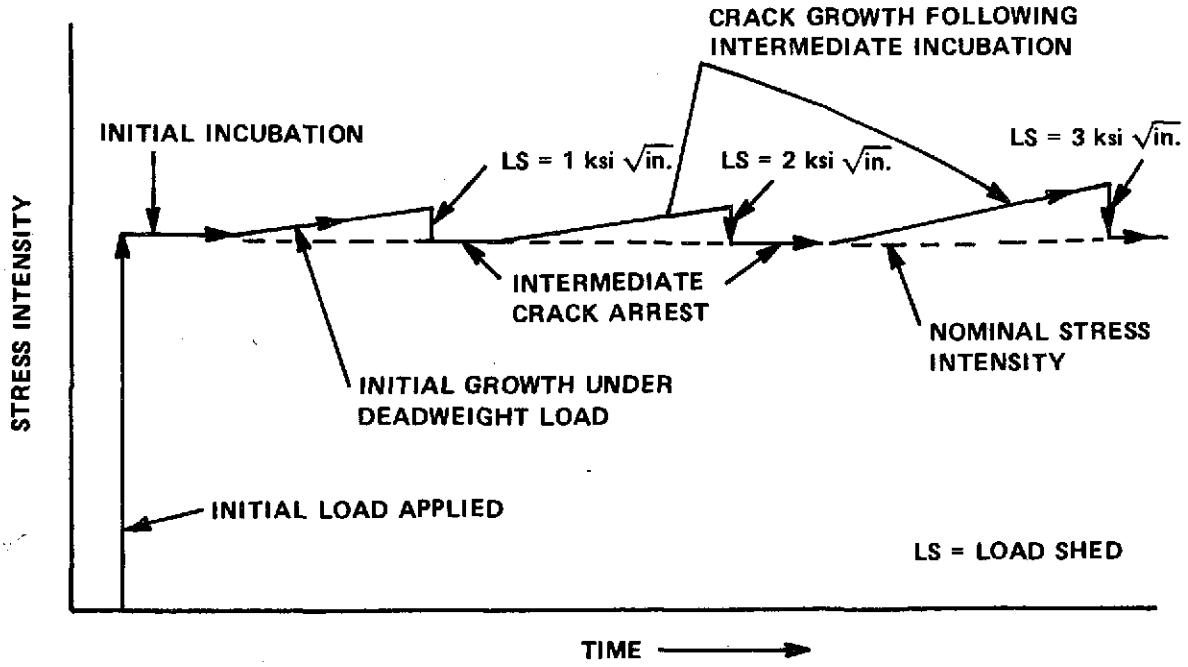

a. Load-shedding sequence not passing through zero load.

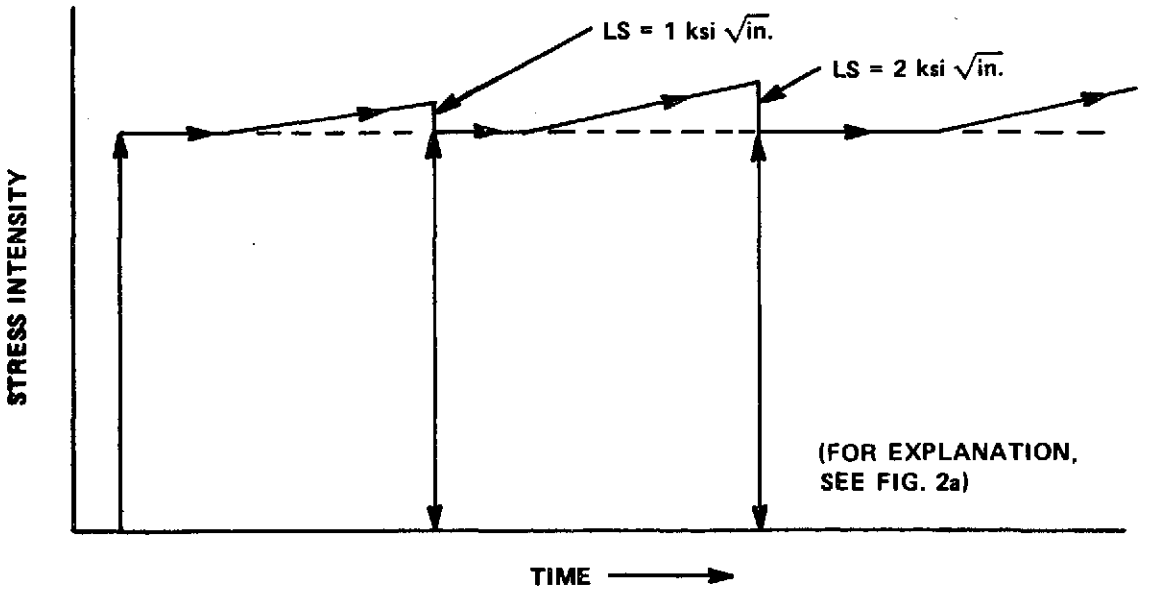

b. Load-shedding sequence passing through zero load.

Figure 2. Flow diagram for stress intensities applied to specimen.

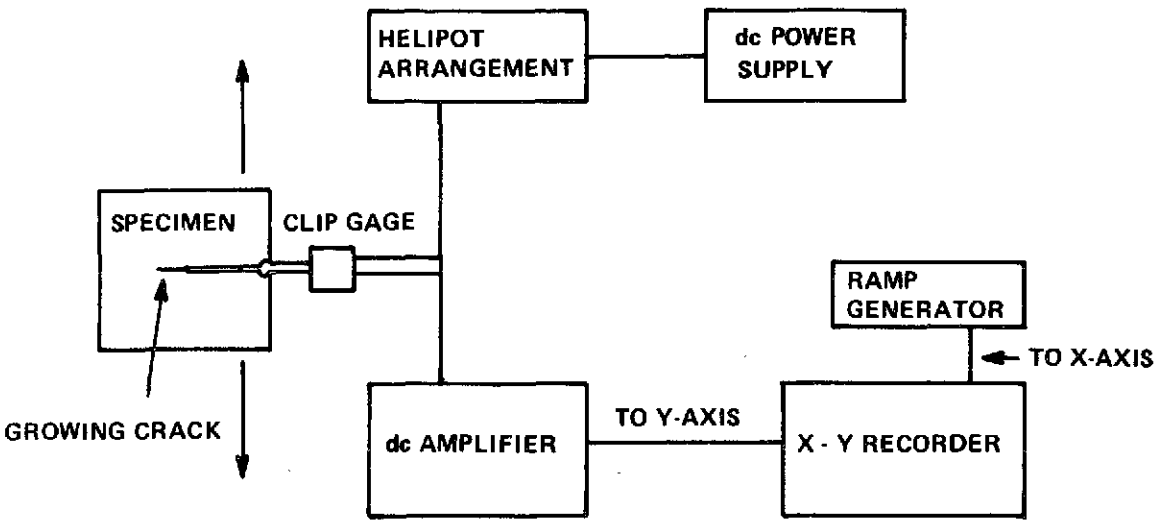

Figure 3. Block diagram of experimental technique.

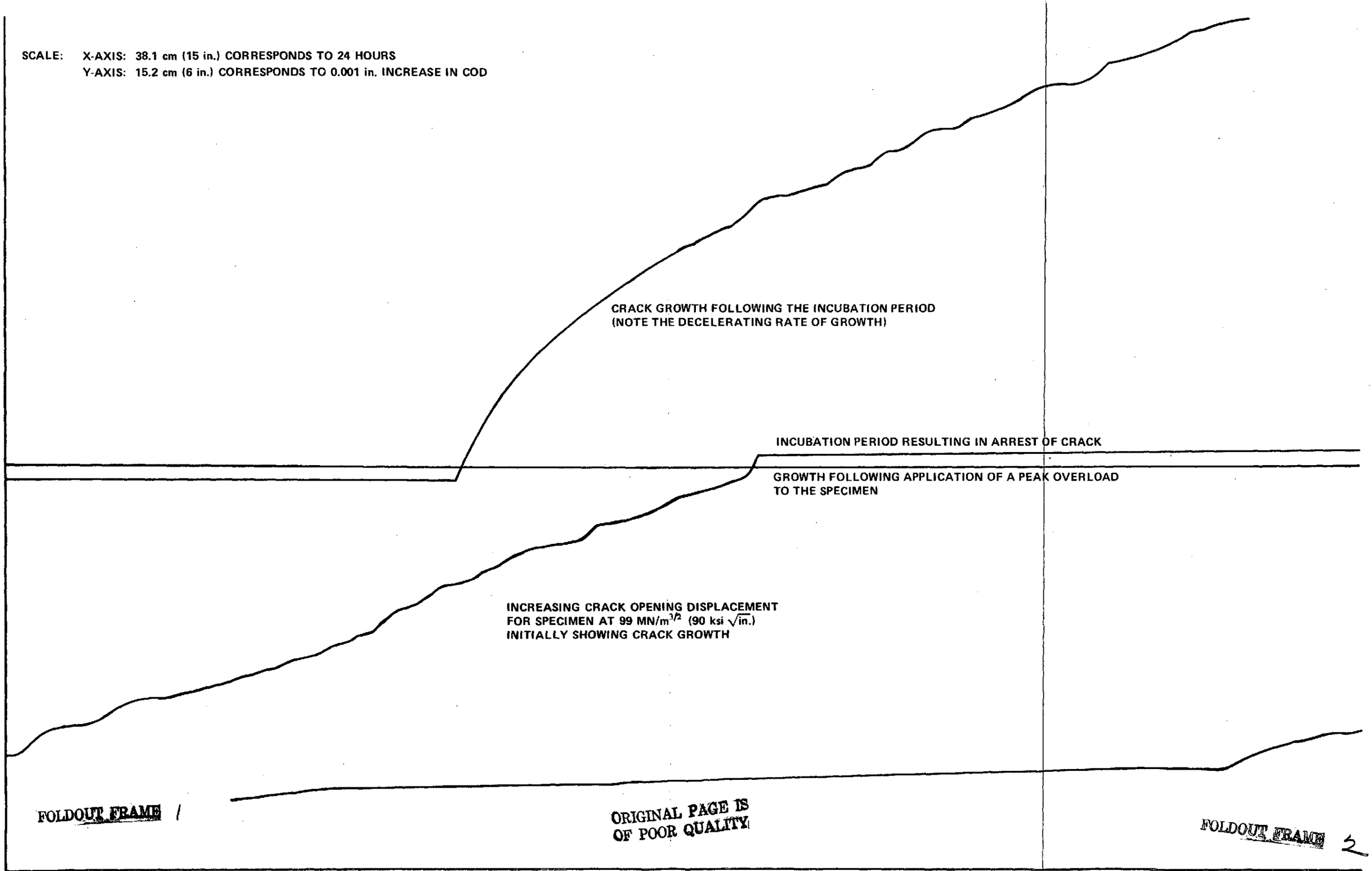

Figure 4. Tracing of recorder plot showing steady-state growth and crack arrest.

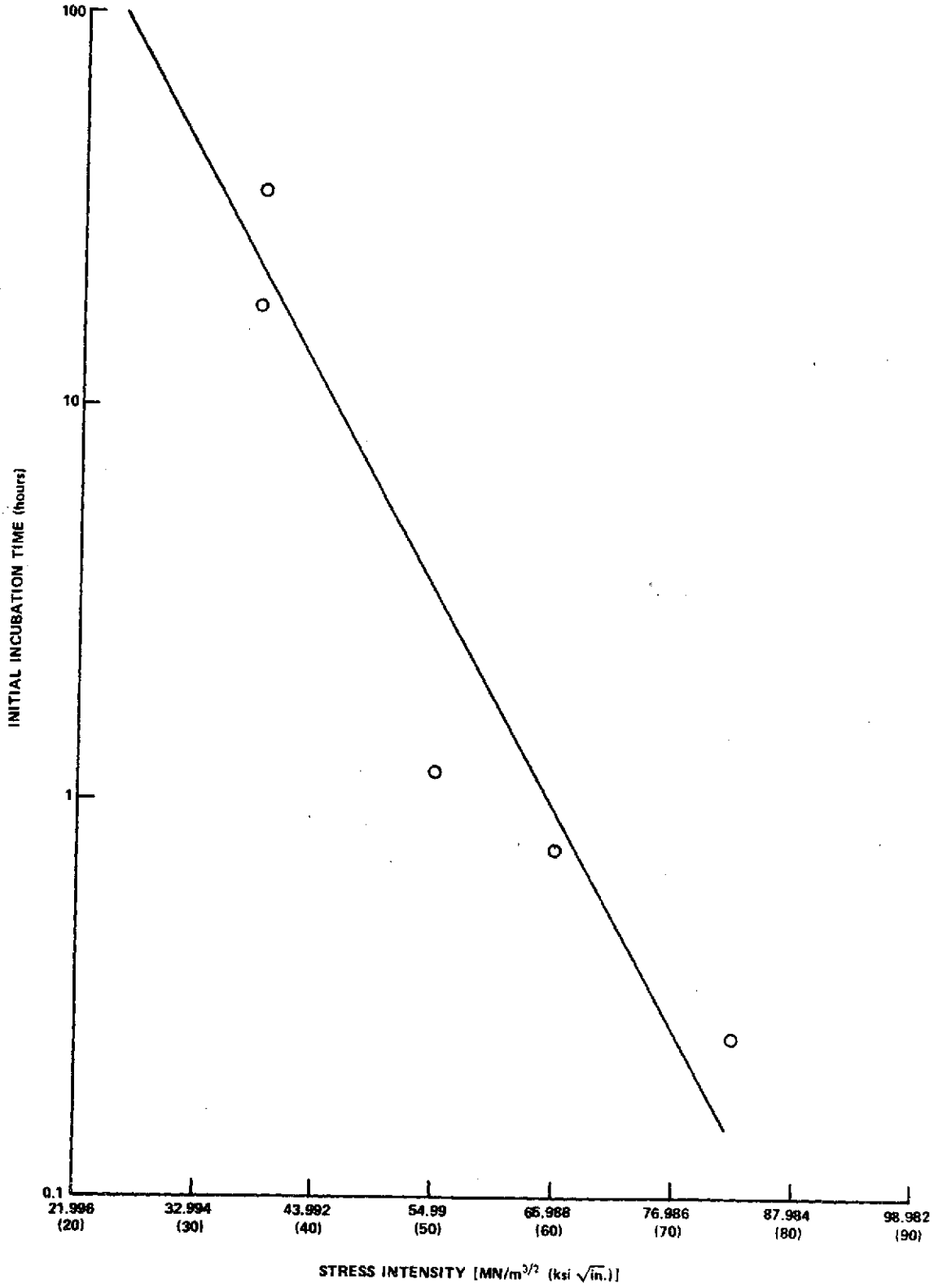

Figure 5. Initial incubation times as a function of initial stress intensity.

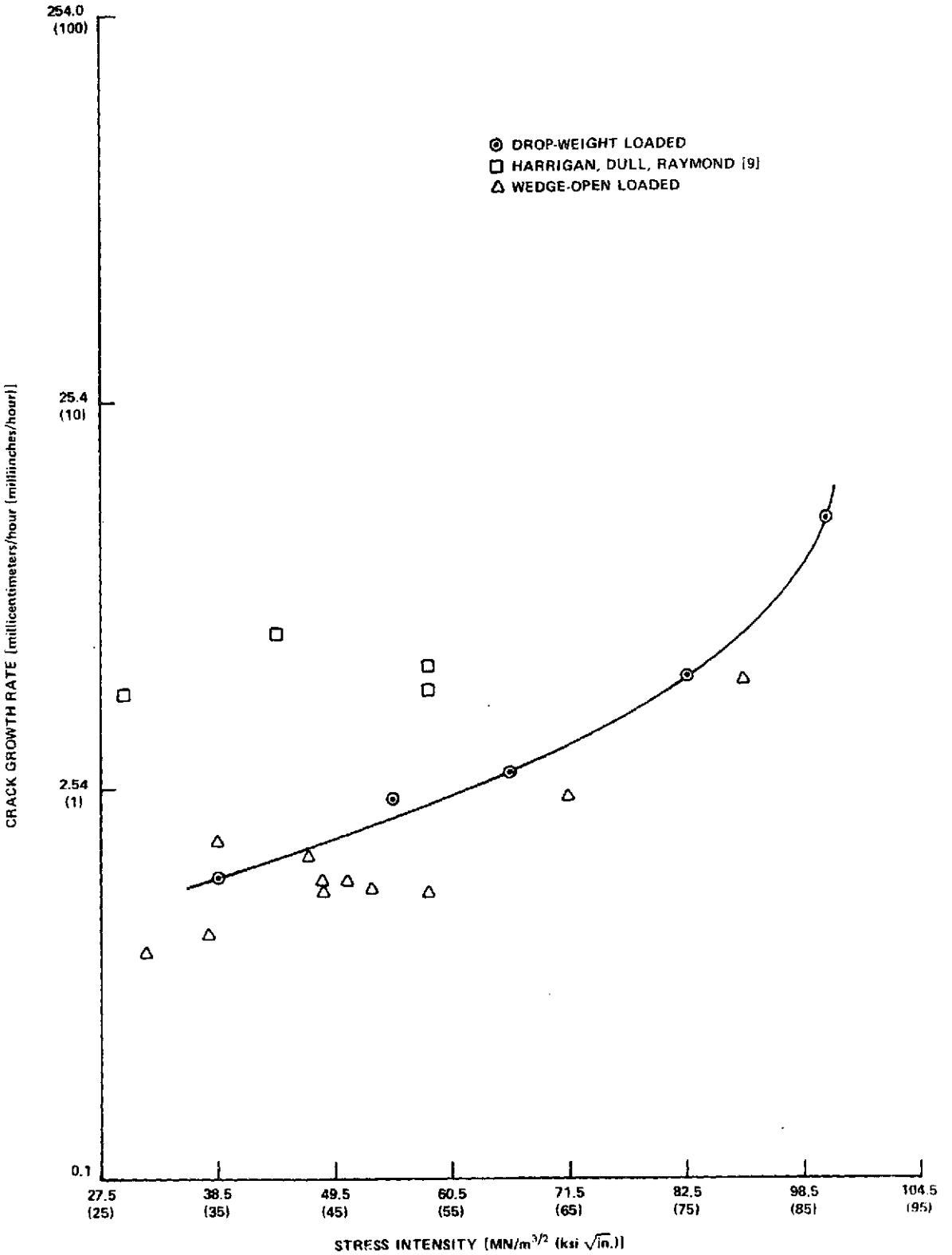

Figure 6. Crack growth rate versus stress intensity in 3.5 percent salt solution.

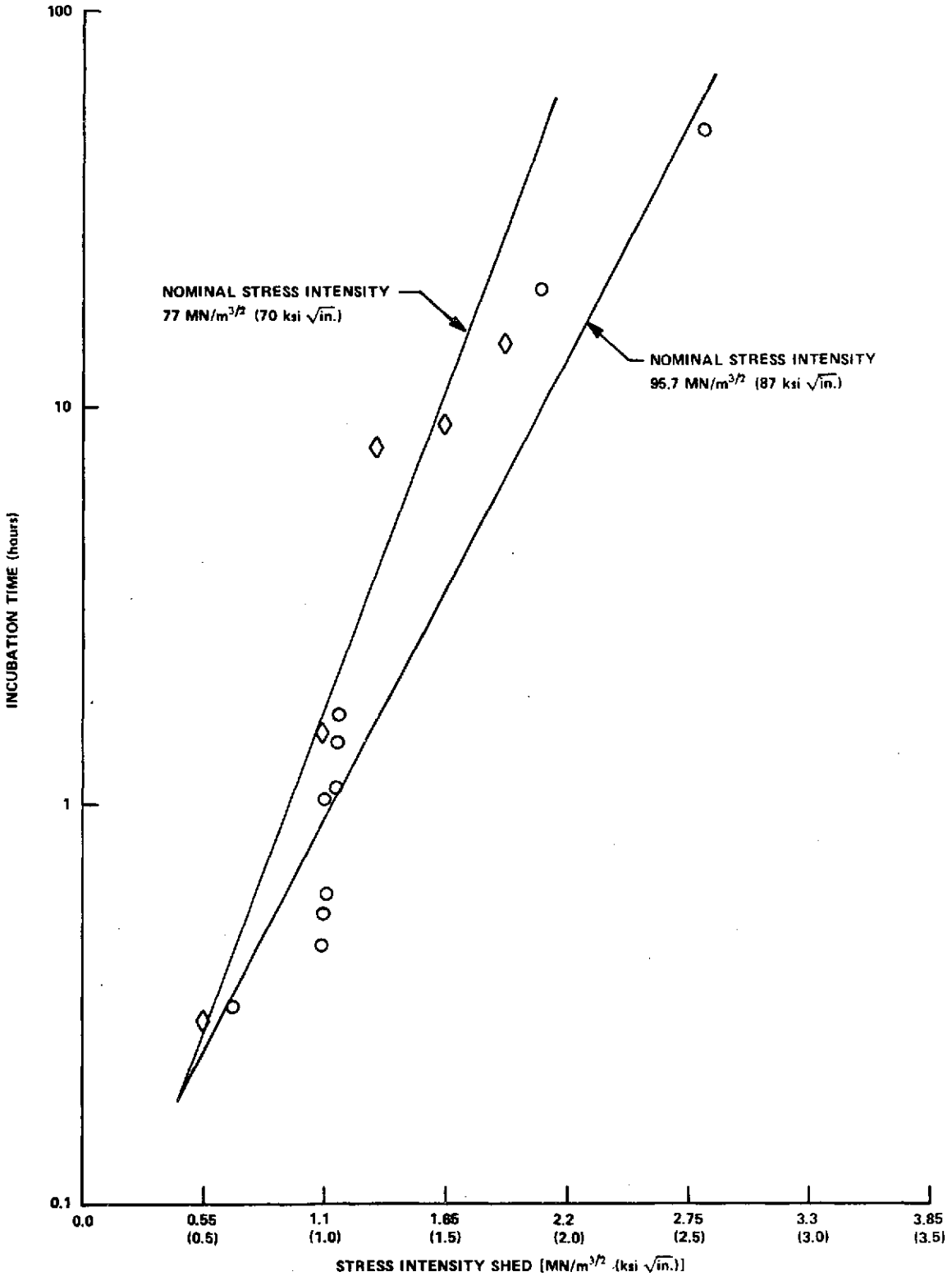

Figure 7. Incubation times for load shed not passing through zero load from a steady-state condition of crack growth.

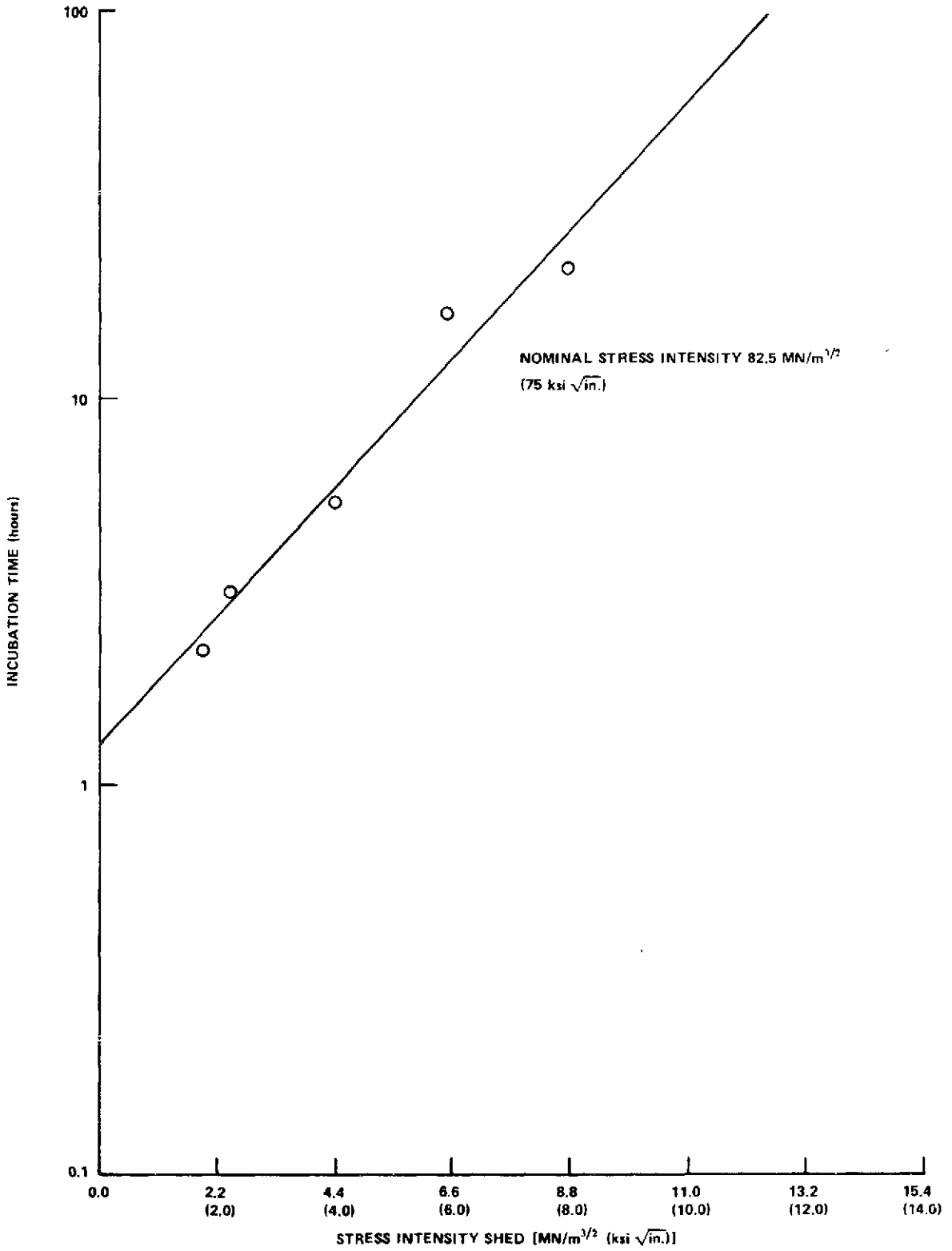

Figure 8. Incubation times for load shed passing through zero load from a steady-state condition of crack growth.

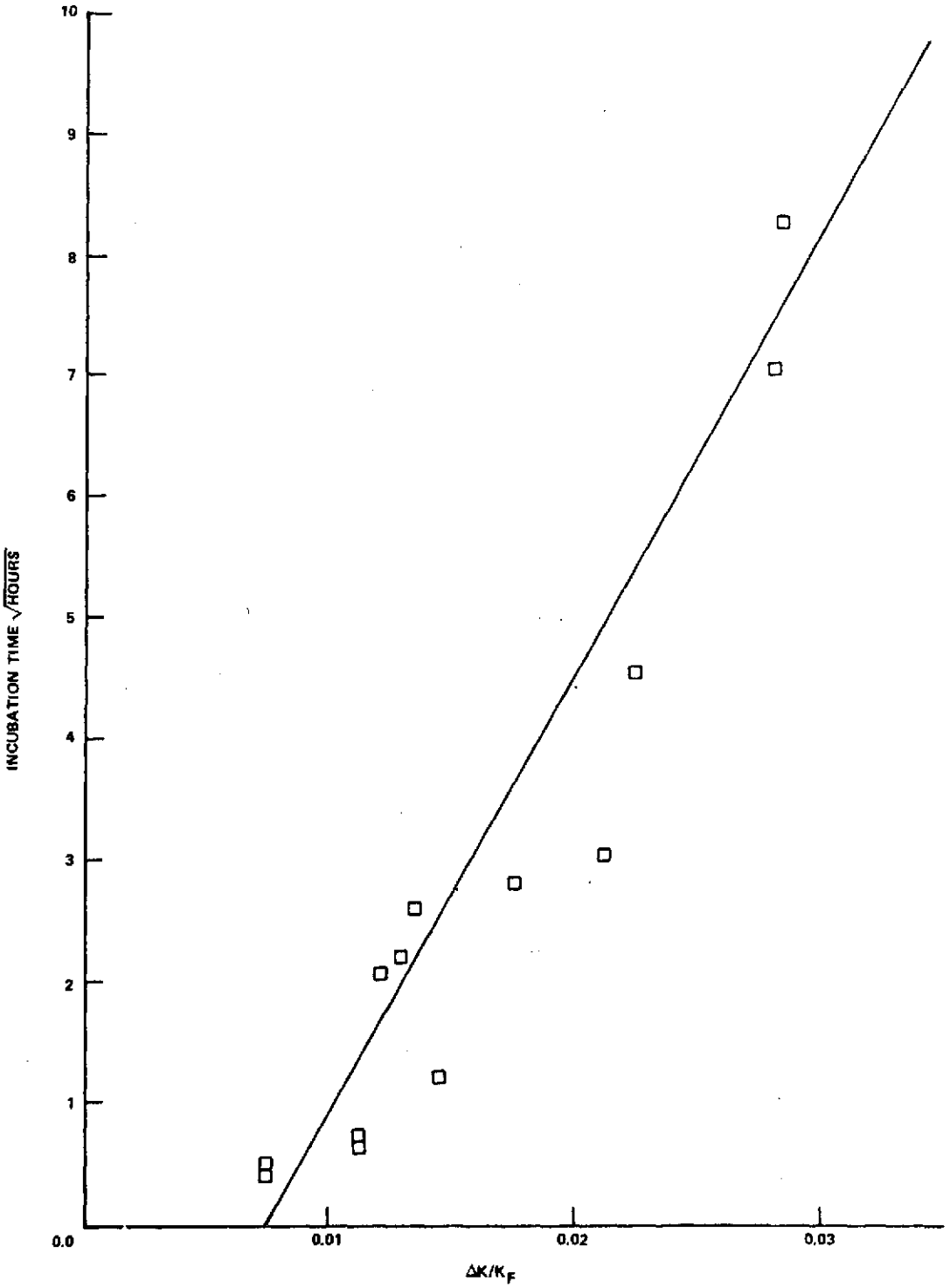

Figure 9. Ratio of stress intensities vs square root of time for incubation after load shedding not passing through zero load.

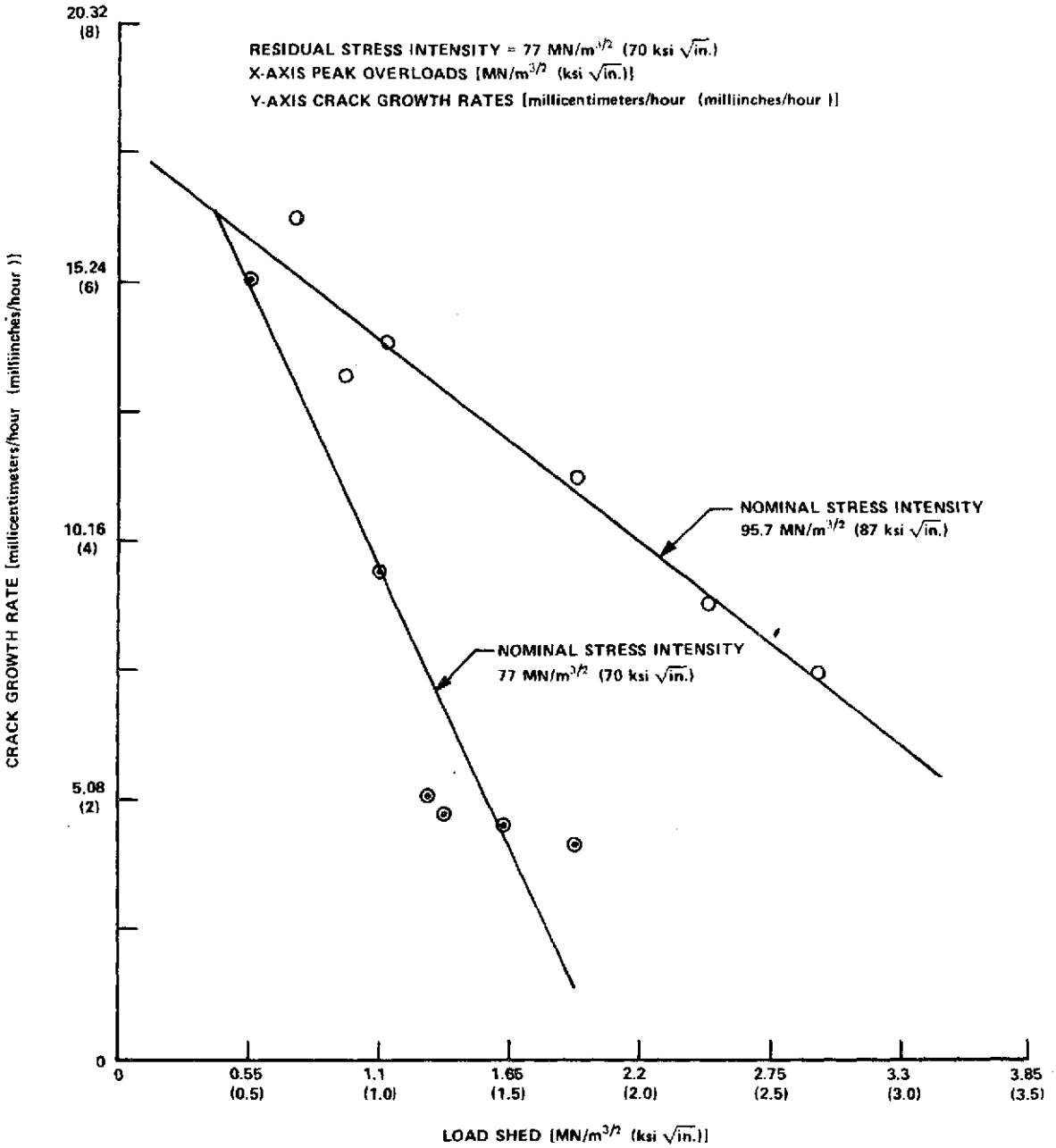

Figure 10. Crack growth rates following incubation vs load shed not passing through zero load.

APPROVAL

KINETIC STUDIES ON THE STRESS CORROSION CRACKING OF D6AC STEEL

By Pascal J. Noronha

The information in this report has been reviewed for security classification. Review of any information concerning Department of Defense or Atomic Energy Commission programs has been made by the MSFC Security Classification Officer. This report, in its entirety, has been determined to be unclassified.

This document has also been reviewed and approved for technical accuracy.

E. C. McKANNAN
Chief, Metallic Materials Division

R. J. SCHWINGHAMER
Director
Materials & Processes Laboratory

DISTRIBUTION

INTERNAL

DA01
Dr. Lucas

DD01
Mr. Smith

EE01
Mr. Kingsbury

EG01
Mr. Brooks

ER01
Dr. Dozier

EC01
Mr. Moore

ES01
Dr. Lundquist

ET01
Mr. Reinartz

ED01
Dr. Lovingood

EL01
Dr. Thomason

EP01
Mr. McCool
Mr. Coldwater

EP41
Mr. Hopson
Mr. Lifer

EF01
Mr. Powell

EH01
Mr. Schwinghamer
Mr. Pace
Mr. Cataldo

EH41
Mr. W. J. Franklin

EH11
Dr. Gause

EH31
Dr. Curry

EH21
Mr. McKannan
Mr. Schuerer

EH22
Mr. Gilmore

EH23
Mr. Hess

EH24
Mr. D. Franklin

AS61 (2)

AS61L (8)

AT01
Mr. Wiggins (6)

CC
Mr. Wofford

EXTERNAL

Scientific and Technical Information
Facility (25)
P.O. Box 33
College Park, MD 20740
Attn: NASA Representative (S-AK/RKT)